Solid Solution Phases with MnP Type Structure: $T_{1-t}Ni_tP$ (T = Ti–Co)

Helmer Fjellvåg and Arne Kjekshus*

Kjemisk Institutt, Universitetet i Oslo, Blindern, N-0315 Oslo 3, Norway

Fjellvåg, Helmer and Kjekshus, Arne. 1986. Solid Solution Phases with MnP Type Structure: $T_{1-t}Ni_tP$ (T = Ti–Co). – Acta Chem. Scand. A 40: 8–16.

The homogeneity ranges of the MnP type solid solution phases $T_{1-t}Ni_tP$ (T = Cr–Co) vary systematically with T, the phase limit for slowly cooled samples being at $t = 0.70 \pm 0.05$ for T = Cr, $t = 0.60 \pm 0.05$ for T = Mn, $t = 0.32 \pm 0.05$ for T = Fe and $t = 0.15 \pm 0.05$ for T = Co. These findings comply with a maximum number of ~14 valence electrons per formula unit for the MnP type structure. No MnP type phase was observed in the TiP–NiP and VP–NiP systems. None of the MnP type phases in the TP–NiP (T = Cr–Co) systems undergo the MnP ⇄ NiAs type transition below 1300 K. It is shown that the magnetic properties of MnP cannot be generated by the isoelectronic, solid solution phases $Cr_{0.50}Fe_{0.50}P$, $Cr_{0.67}Co_{0.33}P$ and $Cr_{0.75}Ni_{0.25}P$.

The monophosphides of the 3*d* metals (T = Ti–Ni) adopt crystal structures which are related to the NiAs type. Only VP does in fact take the (hexagonal) NiAs type structure, but due to its exceptional axial ratio (1.957[1]), which *inter alia* gives rise to 8 (= 6 + 2) short V–V contacts, VP becomes atypical for the NiAs type family. CrP,[2,3] MnP,[2,4] FeP[2,4,5] and CoP[2,4] all take the MnP type structure, which is an orthorhombic, slightly distorted variant of the NiAs type. TiP[6] and NiP[7] crystallize in separate structure types, which, in different ways, are related to the NiAs type structure.

The binary TX (X = P,As,Sb) phases have the general ability to form extended mutual solid solution ranges. This feature is illustrated in Fig. 1 which compares unit cell volumes for different $T_{1-t}T'_tX$ solid solution phases.[8–31] The object of the present communication is to introduce some fresh results for $T_{1-t}Ni_tP$ solid solution phases.

MnP[22,32,33] and FeP[34] are special among the binary TP phases in that they exhibit long range magnetic order at low temperature. A recent study[35] of the $Mn_{1-t}T_tP$ (solid solution) phases has revealed correlation between certain magnetic characteristics (*viz.* moments and co-operative ordering temperatures) and the number of valence electrons. Hence, it seemed worthwhile to check whether valence electron numbers for $T_{1-t}T'_tP$ (T = Ti–Cr; T' = Fe–Ni) corresponding to, say, MnP could give rise to magnetic properties which resemble those of the binary compound. The $T_{1-t}Ni_tP$ phases offer possibilities to test this hypothesis.

Experimental

The ternary samples were made from initial batches of TiP, VP, CrP, MnP, FeP, CoP and "NiP", which, except for TiP, were made as described in Refs. 1, 19, 22, 25–27 (where also the purities of the starting materials are given). TiP was obtained from 99.97 % Ti (sponge; Johnson, Matthey & Co.) and 99.999 % P (lumps of red P; Koch-Light Laboratories) after two heat treatments at 1000 °C with intermediate crushing. The temperature was varied slowly during heating (~150 °C/d) and cooling, and the samples were kept at the maximum temperature for 5 d. Ternary $T_{1-t}Ni_tP$ samples were synthesized by heating weighed amounts of the appropriate binary compounds in evacuated, sealed silica tubes. All

*To whom correspondence should be addressed.

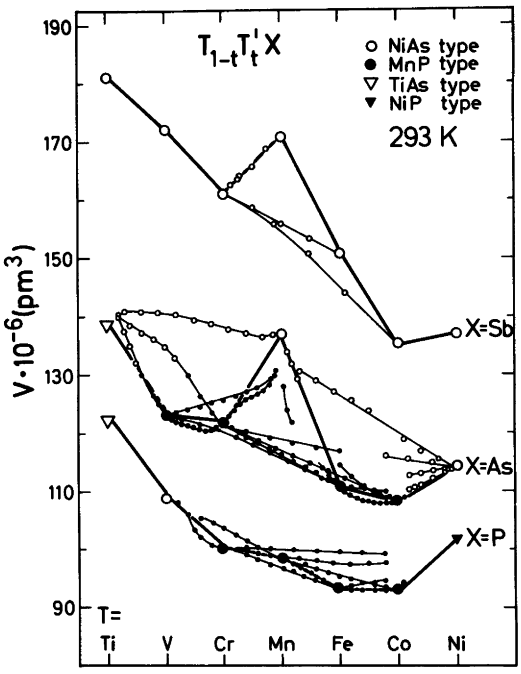

Fig. 1. Unit cell volume (per 4 $T_{1-t}T'_tX$ formula units as for the MnP type structure) for different $T_{1-t}T'_tX$ solid solution phases. Legends to symbols for different structure types are given on the illustration. Thicker lines join binary phases with Vegard law relationships, narrower curves connect expermental points for ternary solid solution phases. Data from Refs. 1–31.

samples were generally subjected to three heat treatments (each of 7 d duration), interrupted by cooling to room temperature and careful grinding. However, the annealing temperatures (in the range 800 to 1000 °C) were individually selected for the different ternary phases. The samples were finally brought to 800 °C and either cooled slowly to room temperature (over 2–4 d) or quenched in ice water.

$Cr_{0.50}Fe_{0.50}P$ was prepared as described in Ref. 19. $Cr_{0.67}Co_{0.33}P$ was synthesized from CrP and CoP by a heat treatment at 850 °C for 4 d, followed by 4 d at 1000° and cooling to room temperature over 2 d. After careful grinding the $Cr_{0.67}Co_{0.33}P$ samples were then reannealed at 900 °C for 7 d and finally cooled to room temperature over 4 d.

All samples were characterized at room temperature by powder X-ray diffraction (Guinier technique, $CuK\alpha_1$ radiation, Si as internal standard). Low and high temperature X-ray diffraction photographs were taken with a Guinier Simon camera (Enraf-Nonius FR 553) between 100 and 1300 K. Unit cell dimensions were obtained through least squares refinements of the positions of 15–25 well defined Bragg reflections. Powder X-ray diffraction intensity data were deduced from the Guinier photographs by means of a Nicolet filmscanning system L 18. The integrated intensities obtained in this way were least squares processed by the programme SHELX[36] to extract values for the positional parameters of the metal and non-metal atoms.

Powder neutron diffraction diagrams of $Cr_{0.50}Fe_{0.50}P$ at 293 and 10 K (Displex cooling device) were recorded with the OPUS III spectrometer at the JEEP II reactor, Kjeller, using neutrons of wavelength 187.7 pm. The Hewat[37] version of the Rietveld [38] programme was used in the profile refinements of the powder neutron diffraction data. The scattering lengths (in 10^{-12} cm) $b_{Cr} = 0.3635$, $b_{Fe} = 0.954$ and $b_P = 0.513$ were taken from Ref. 39.

Magnetic susceptibility data were recorded with a conventional Faraday balance (maximum field ~8 kOe; 20–35 mg samples) between 80 and 1000 K. Differential scanning calorimetry (DSC) was performed between 100 and 900 K using a Mettler TA 3000 system.

Results and discussion

(i) *Homogeneity ranges and structural data.* MnP type solid solution phases were identified in the CrP–NiP, MnP–NiP, FeP–NiP and CoP–NiP systems. The TiP–NiP and VP–NiP systems exhibit no phase with the MnP type structure, and only minor amounts of NiP can be dissolved in TiP and VP. Phases with the NiP type structure reported by Larsson[7] were not observed in any of the *T*P–NiP systems (*cf.* the more detailed account for the MnP–NiP system in Ref. 26). Since the main concern of the present study was the MnP and/or NiAs type phases, no efforts were made to pursue the indications which have been obtained for the existence of additional intermediate phases in the VP–NiP, FeP–NiP and CoP–NiP systems.

Fig. 2 shows the compositional variations of the unit cell dimensions for the $Cr_{1-t}Ni_tP$, $Fe_{1-t}Ni_tP$ and $Co_{1-t}Ni_tP$ phases with MnP type

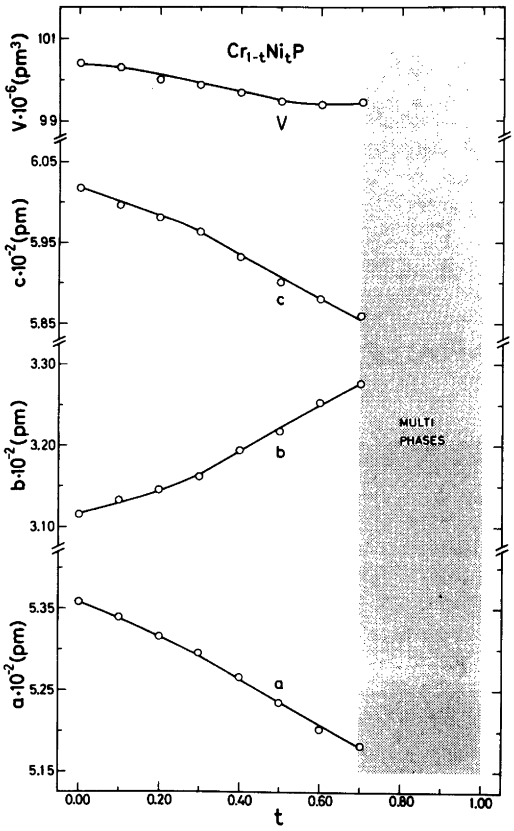

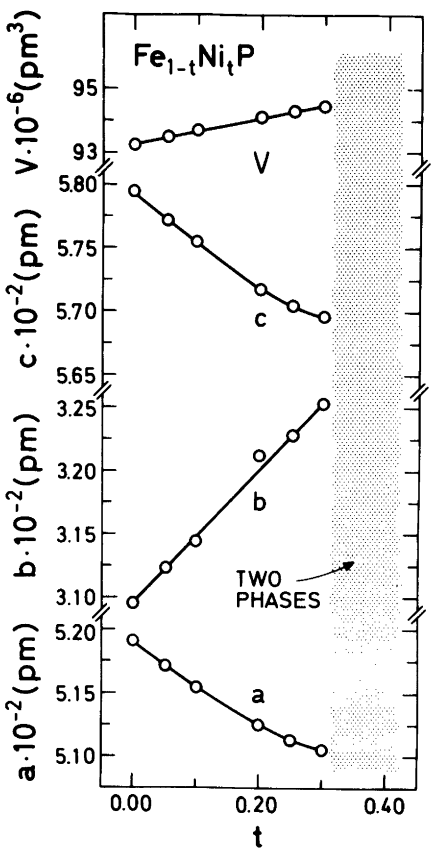

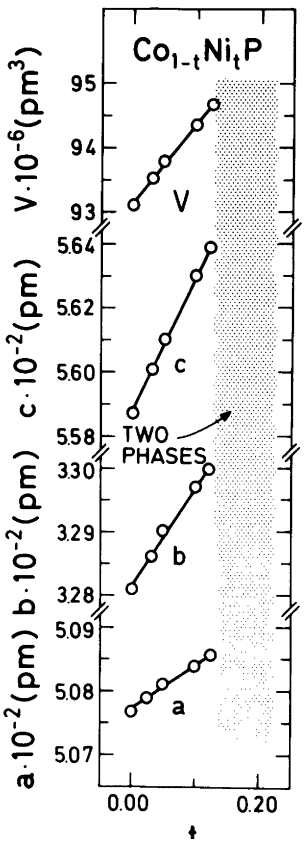

Fig. 2. Unit cell dimensions (at 293 K) *versus t* for (a) $Cr_{1-t}Ni_tP$, (b) $Fe_{1-t}Ni_tP$ and (c) $Co_{1-t}Ni_tP$. *Calculated* error limits do not exceed size of symbols.

structure (using *Pnma* setting, $c > a > b$), and corresponding data for $Mn_{1-t}Ni_tP$ are given in Ref. 26. (Fig. 2 refers to results obtained at room temperature for slowly cooled samples, but systematic distinctions were not disclosed for the samples which were quenched from 800 °C.) The homogeneity ranges of these solid solution phases decrease in the order $Cr_{1-t}Ni_tP$ ($0.00 \leqq t \leqq 0.70 \pm 0.05$), $Mn_{1-t}Ni_tP$ ($0.00 \leqq t \leqq 0.60 \pm 0.05$[26]), $Fe_{1-t}Ni_tP$ ($0.00 \leqq t \leqq 0.32 \pm 0.05$) and $Co_{1-t}Ni_tP$ ($0.00 \leqq t \leqq 0.15 \pm 0.05$). The situation is somewhat similar for the $T_{1-t}Ni_tAs$ series where the phase limits are $t = 0.50 \pm 0.05$ for $T = Cr$,[17] $t = 0.65 \pm 0.05$ (including the region with superstructural ordering perturbed on the basic NiAs/MnP type atomic arrangement) for $T = Mn$,[31] $t = 0.40 \pm 0.05$ for $T = Fe$[17] and $t = 0.12 \pm 0.02$ for $T = Co$.[23]

Fig. 3 illustrates the systematic variation in the phase limit for the $T_{1-t}Ni_tP$ and $T_{1-t}Ni_tAs$ phases

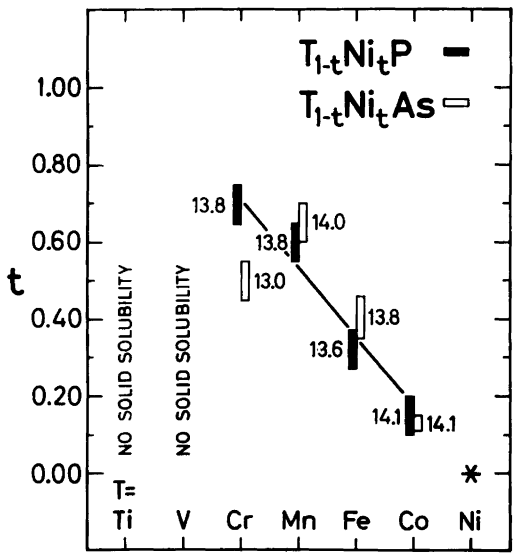

Fig. 3. Limit for MnP type solid solution phases of $T_{1-t}Ni_tP$ and $T_{1-t}Ni_tAs$ (T = Ti–Co). Data for arsenides are taken from Refs. 17, 23, 31. Numbers give valence electrons (see text) per formula unit. Line is guide for the eye.

with T. The deviation for $Cr_{1-t}Ni_tAs$ from the trend may suggest that the homogeneity range for this phase can be extended somewhat at optimum annealing conditions. The binary MnP type compounds (*cf.*, *e.g.*, the listing in Ref. 40) extend from 10 to 14 valence electrons per TX unit, counting ns^2 and $(n-1)d^i$ for T and ns^2 and np^j for X as valence electrons. As seen from the number of valence electrons per formula unit given on Fig. 3, the upper valence electron limit is nicely confirmed by the phase boundaries for $T_{1-t}Ni_tP$ and $T_{1-t}Ni_tAs$. The lower valence electron limit also shows up for ternary phases, but the evidences are here limited to $V_{1-t}Ti_tAs$ and $Cr_{1-t}Ti_tAs$ with 9.5 and 10.2 valence electrons per formula unit, respectively.[29,30] These yet empirical facts appear to receive some support from the electronic band structures and densities of states calculated for the TP series by Perkins *et al.*,[41] which show that essentially complete filling of the T 3*d* bands is reached at CoP (*viz.* 14 valence electrons per formula unit). On the other hand, it should perhaps be remembered that the electronic band structure is not the only factor which "governs" the occurrence of the MnP type structure. The relative atomic sizes of the components (*cf.* Refs. 42, 43) enter also as a controlling factor for the total free energy.

A question which often arises in connection with MnP type phases is whether a transition to the NiAs type structure as a function of temperature will occur. $c/b = \sqrt{3}$ serves as a necessary (but not sufficient) condition for the occurrence of an MnP to NiAs type transition. Since there are appreciable changes in c/b with t at room temperature for $Cr_{1-t}Ni_tP$ (c/b = 1.933 for t = 0.00; c/b = 1.789 for t = 0.70) and $Fe_{1-t}Ni_tP$ (c/b = 1.869 for t = 0.00; c/b = 1.750 for t = 0.30) the possibility of structural phase transitions in these phases at higher temperatures was checked. High temperature powder X-ray data were accordingly collected for $Cr_{1-t}Ni_tP$ with t = 0.30, 0.50 and 0.70 and $Fe_{1-t}Ni_tP$ with t = 0.30. However, the resulting thermal expansion curves (Fig. 4) show that c/b varies only slightly with the temperature and there is no indication of any phase transition in these samples.

Positional parameters for $Cr_{1-t}Ni_tP$ with t = 0.10, 0.30, 0.50 and 0.70 were obtained through least squares refinements of powder X-ray diffraction data. [Cr and Ni were assumed randomly (long range) distributed over the T sublattice; T in 4*c* and P in 4*c* of space group *Pnma*.] The values for the positional parameters thus obtained are constant within two calculated standard deviations, but the magnitudes of the standard deviations are about three to four times larger than those derived by neutron diffraction for the natural reference compound CrP.[3] However, averaging of the individual sets of values leads to positional parameters with associated standard deviations [x_T = 0.0088(9), z_T = 0.1979(8); x_P = 0.1871(12), z_P = 0.5637(11)] which compare favourably with those for CrP.

Hence, according to both the positional parameters at room temperature and the thermal expansion properties below 1300 K, $Cr_{1-t}Ni_tP$ do not satisfy the conditions for an MnP to NiAs type phase transition. The natural question is then: what are the conditions for such a transition? Some aspects of an answer to this question are incorporated into the geometrical model discussed in Refs. 42, 43. Another way to elucidate the problem is to consider the relationship betwen the average T–X bond distance ($d_{T-X,\,average}$) and the unit cell volume (V) for phases with the MnP and NiAs type structures. Fig. 5

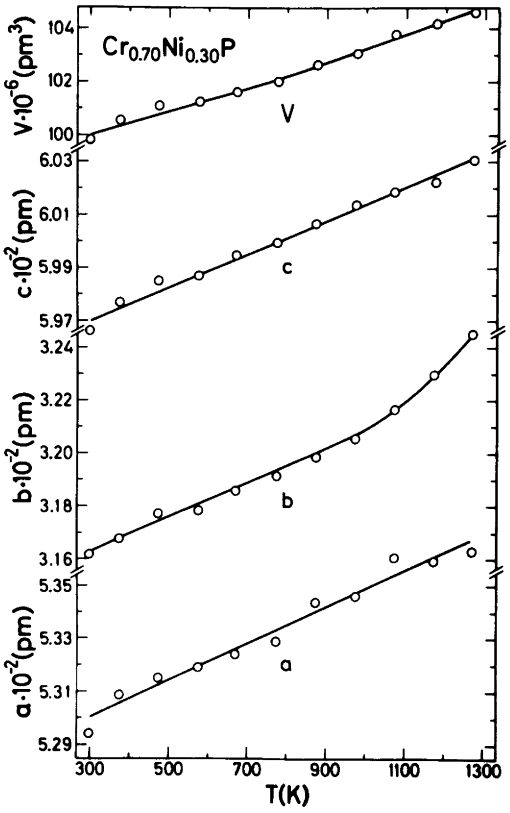

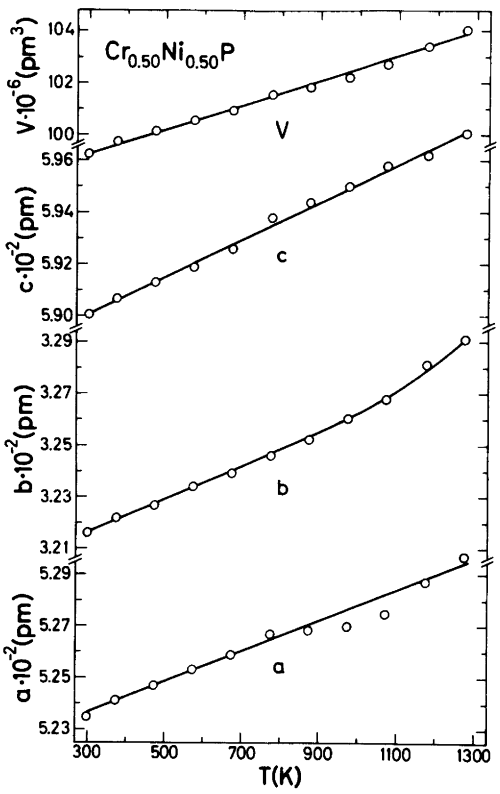

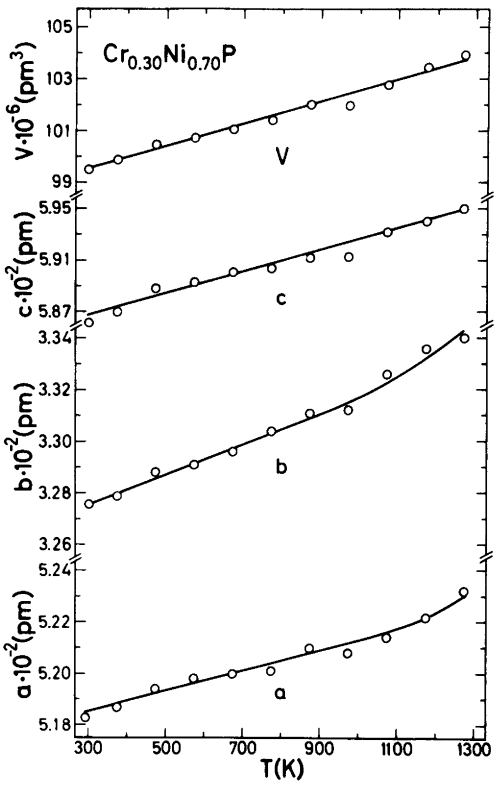

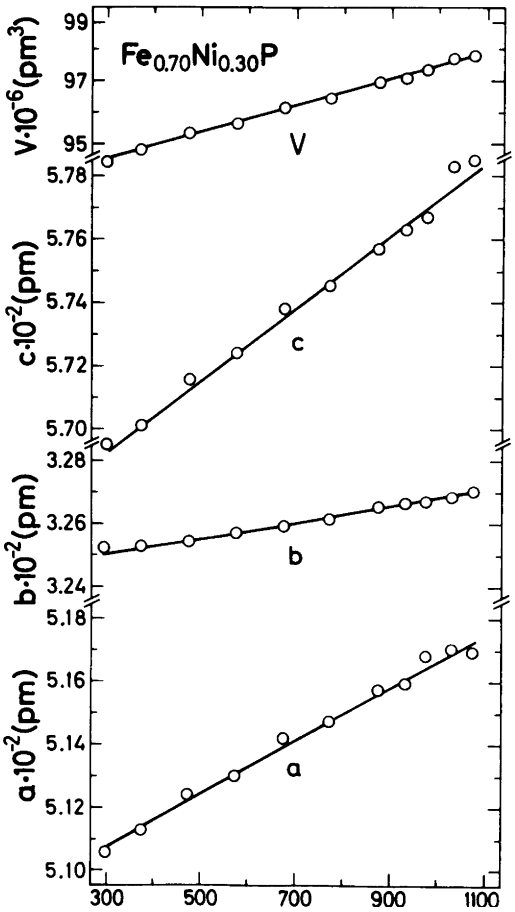

Fig. 4. Unit cell dimensions *versus* temperature for (a) $Cr_{0.70}Ni_{0.30}P$, (b) $Cr_{0.50}Ni_{0.50}P$, (c) $Cr_{0.30}Ni_{0.70}P$ and (d) $Fe_{0.70}Ni_{0.30}P$ between 300 and 1300 K. Calculated error limits do not exceed the size of symbol.

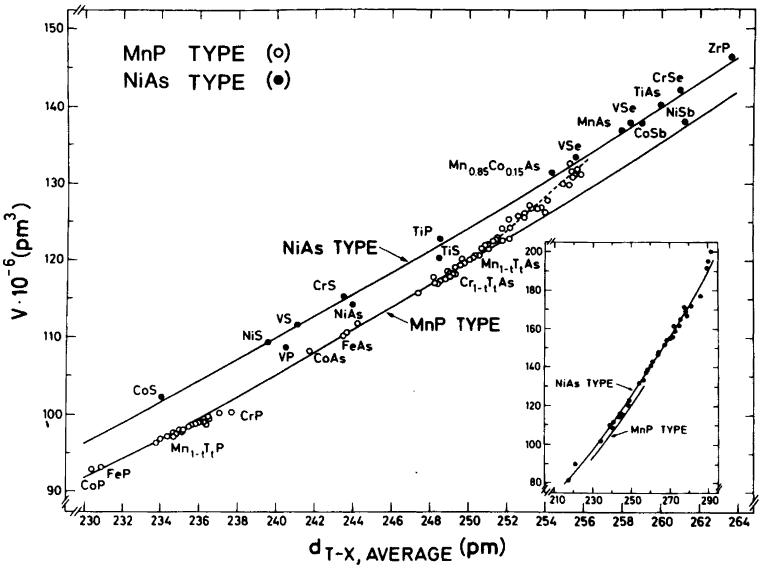

Fig. 5. Average *T–X* bond distance *versus* unit cell volume (per four formula units as for the MnP type structure) for binary and ternary MnP and NiAs type phases. Data from Refs. 1–31, 40. Solid curves are calculated numerically as described in the text.

shows that there is a distinct correlation between these quantities (as measured at room temperature), and moreover that the experimental points nicely follow the curves obtained through numerical model calculations. The computations for the NiAs type structure were performed by varying c_{NiAs} in steps of 5 over $520 \leqq c_{NiAs} \leqq 625$ pm and $(c/a)_{NiAs}$ in steps of 0.05 over $1.25 \leqq (c/a)_{NiAs} \leqq 2.00$, covering the entire parameter field mentioned. The variable positional parameters of the MnP type structure were fixed at $x_T = 0.005$, $z_T = 0.200$, $x_X = 0.200$ and $z_X = 0.578$ (*viz.* the parameters specifying the "idealized" MnP type structure, *cf.* Refs. 42, 43) in the computations for the MnP type structure, where c_{MnP} was varied in steps of 0.05 over $550 \leqq c_{MnP} \leqq 620$ pm, $(c/a)_{MnP}$ in

Table 1. Structural data for MnP (quoted from Ref. 22), $Cr_{0.50}Fe_{0.50}P$ (neutron diffraction) $Cr_{0.67}Co_{0.33}P$ (X-ray diffraction) and $Cr_{0.75}Ni_{0.25}P$ (X-ray diffraction) at 293 K.

Phase	MnP	$Cr_{0.50}Fe_{0.50}P$[a]	$Cr_{0.67}Co_{0.33}P$	$Cr_{0.75}Ni_{0.25}P$
a (pm)	526.01(4)	527.70(5)	532.71(9)	530.33(8)
b (pm)	317.41(2)	310.32(3)	312.08(7)	315.28(5)
c (pm)	591.27(4)	591.68(6)	599.48(10)	597.51(7)
$V \times 10^{-6}$ (pm³)	98.72(2)	96.89(3)	99.66(5)	99.90(5)
x_T	0.0061(11)	0.0058(16)	0.005(3)	0.007(3)
z_T	0.1962(12)	0.1967(12)	0.196(2)	0.199(2)
x_P	0.1884(8)	0.1882(18)	0.188(3)	0.187(2)
z_P	0.5690(7)	0.5691(16)	0.572(2)	0.566(2)
$d_{T-P,\,average}$ (pm)	235.7	234.4	236.7	236.3
$d_{1,4}$ (pm)	270.6(3)	271.3(3)	274(1)	272(1)
$d_{2,1}$ (pm)	281.2(12)	279.8(12)	282(2)	285(2)

[a] $a = 527.21(5)$ pm, $b = 309.25(3)$ pm, $c = 591.06(6)$ pm, $V = 96.37(3) \times 10^6$ pm³; $x_T = 0.0044(17)$, $z_T = 0.1966(11)$, $x_P = 0.1869(17)$, $z_P = 0.5670(15)$ at 10 K.

steps of 0.01 over $1.08 \leqq (c/a)_{MnP} \leqq 1.16$ and $(c/b)_{MnP}$ in steps of 0.05 over $1.60 \leqq (c/b)_{MnP} \leqq 1.95$. [All points of the c_{MnP}, $(c/a)_{mnf}$, $(c/b)_{MnP}$ parameter space were covered.] The $d_{T-X,average}$ *versus* V relationships thus obtained trace out virtually parallel curves for the MnP and NiAs type structures. The volume difference for a given $d_{T-X,average}$ amounts to $\sim 5\times10^6$ pm^3, and Fig. 5 serves to visualize that the MnP type structure represents a more volume efficient packing than the NiAs type. The larger permitted span in size variation between the T and X components for the latter structure type is evident from the inset. There are remarkably few of the experimental points in Fig. 5 which seriously deviate from the calculated curve profiles. There are admittedly quite a few departures with the MnP type structure, but they are all easily explained since they refer to the $Mn_{1-t}T_tAs$ phases which undergo the MnP ⇄ NiAs type transition just above room temperature.[10,14,15,17,18] The special rank of VP among the NiAs type phases is mentioned in the introduction and this is reflected in its intermediate position in Fig. 5. Similar considerations apply to TiS, whereas the departures for NiAs and in particular NiSb will require quite a different explanation. Returning then to the $T_{1-t}Ni_tP$ phases their combinations of $d_{T-X,average}$ and V values confirm that the MnP ⇄ NiAs type transition is not likely to occur in these phases.

(ii) *Isoelectronic phases with MnP.* Solid solution phases which are isoelectronic and isostructural with MnP occur *inter alia* for $Cr_{0.50}Fe_{0.50}P$, $Cr_{0.67}Co_{0.33}P$ and $Cr_{0.75}Ni_{0.25}P$. It seemed pertinent to check whether these compositions give rise to properties which correspond to those observed for MnP itself.

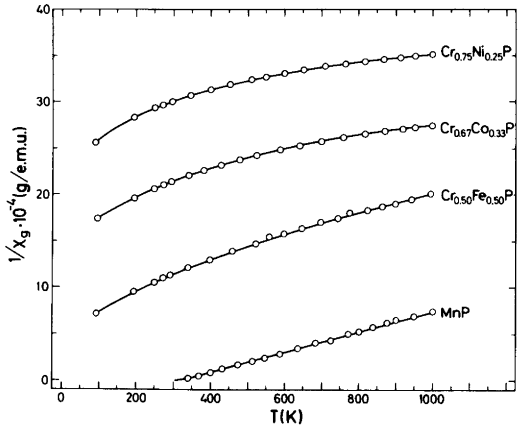

Fig. 6. Inverse magnetic susceptibility *versus* temperature for MnP, $Cr_{0.50}Ni_{0.50}P$, $Cr_{0.67}Co_{0.33}P$ and $Cr_{0.75}Ni_{0.25}P$.

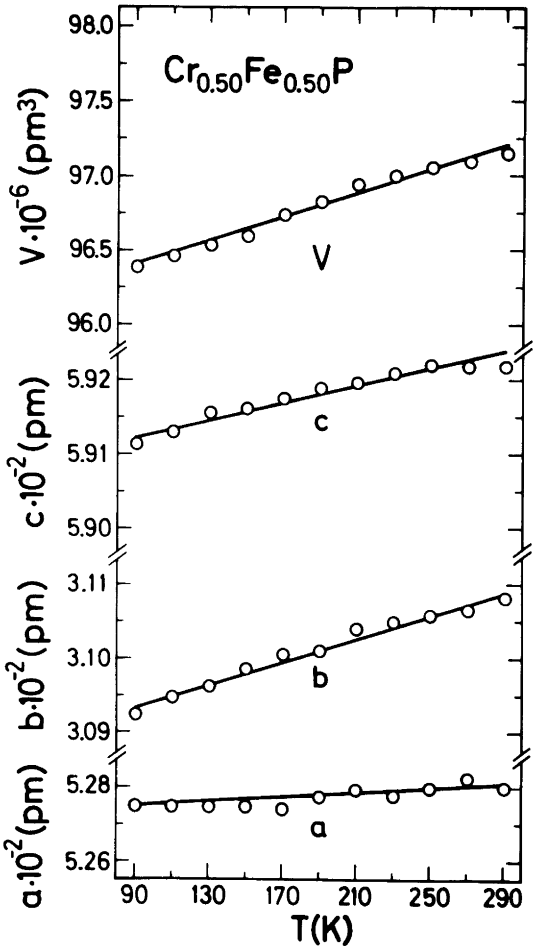

Fig. 7. Unit cell dimensions *versus* temperature for $Cr_{0.50}Fe_{0.50}P$ (90-300 K). *Calculated* error limits do not exceed the size of symbols.

Crystal structure data for MnP (from Ref. 22), $Cr_{0.50}Fe_{0.50}P$ (based on powder neutron diffraction data), $Cr_{0.67}Co_{0.33}P$ and $Cr_{0.75}Ni_{0.25}P$ (the two latter based on powder X-ray diffraction data) are given in Table 1. The table also includes the average T–P bond distance and the shortest T–T distances $d_{1,4}$ and $d_{2,1}$ which are believed to be key quantities for the magnetic properties of MnP

type phases. The main message of Table 1 is that although some of the structural characteristics (*i.e.* the positional parameters) of the isoelectronic phases resemble those of MnP in a somewhat casual way, the dissimilarities (*i.e.* the unit cell dimensions and interatomic distances) are more striking than the similarities.

MnP satisfies the Curie-Weiss law in the paramagnetic state above its Curie temperature T_C = 291 K (*cf.* Ref. 22). As seen from Fig. 6 neither $Cr_{0.50}Fe_{0.50}P$, $Cr_{0.67}Co_{0.33}P$ nor $Cr_{0.75}Ni_{0.25}P$ fulfil the Curie-Weiss law over any extended range of temperature. Moreover, according to Fig. 6 none of the isoelectronic phases exhibit a para- to ferromagnetic transition in the range 80 to 300 K. The lack of magnetic or any other phase transition in $Cr_{0.50}Fe_{0.50}P$, $Cr_{0.67}Co_{0.33}P$ and $Cr_{0.75}Ni_{0.25}P$ between 80 and 300 K is also confirmed by DSC and low temperature powder X-ray diffraction (the results for $Cr_{0.50}Fe_{0.50}P$ being shown in Fig. 7 as an example). These findings are also confirmed by the neutron diffraction examination of $Cr_{0.50}Fe_{0.50}P$, which show that the MnP type structure is retained down to 10 K and that the neutron diffraction patterns contain no contributions of magnetic origin. (Structural data for $Cr_{0.50}Fe_{0.50}P$ at 10 K are given in a footnote to Table 1.)

References

1. Selte, K., Kjekshus, A. and Andresen, A. F. *Acta Chem. Scand. 26* (1972) 4057.
2. Rundqvist, S. and Nawapong, P. C. *Acta Chem. Scand. 19* (1965) 1006.
3. Selte, K., Kjekshus, A. and Andresen, A. F. *Acta Chem. Scand. 26* (1972) 4188.
4. Rundqvist, S. *Acta. Chem. Scand. 16* (1962) 287.
5. Selte, K. and Kjekshus, A. *Acta Chem. Scand. 26* (1972) 1276.
6. Brauer, G., Gingerich, K. and Knausenberger, M. *Angew. Chem. 76* (1964) 187.
7. Larsson, E. *Arkiv Kemi 23* (1964) 335.
8. Takai, W. J., Cox, D. E. and Shirane, G. *Phys. Rev. 129* (1963) 2008.
9. Yamaguchi, K., Watanabe, H., Yamamoto, H. and Yamaguchi, Y. *J. Phys. Soc. Jpn. 31* (1971) 1042.
10. Selte, K., Kjekshus, A. and Andresen, A. F. *Acta Chem. Scand. A 28* (1974) 61.
11. Selte, K., Kjekshus, A. and Oftedal, T. A. *Acta Chem. Scand. A 28* (1974) 803.
12. Selte, K., Hjersing, H., Kjekshus, A. and Andresen, A. F. *Acta Chem. Scand. A 29* (1975) 312.
13. Selte, K., Kjekshus, A. Aaby, S. and Andresen, A. F. *Acta Chem. Scand. A 29* (1975) 810.
14. Selte, K., Kjekshus, A., Valde, G. and Andresen, A. F. *Acta Chem. Scand. A 30* (1976) 8.
15. Selte, K., Kjekshus, A., Valde, G. and Andresen, A. F. *Acta Chem. Scand. A 30* (1976) 468.
16. Andreassen, I. L., Selte, K. and Kjekshus, A. *Acta Chem. Scand. A 31* (1977) 421.
17. Delphin, I. L. A., Selte, K., Kjekshus, A. and Andresen, A. F. *Acta Chem. Scand. A 32* (1978) 179.
18. Selte, K., Kjekshus, A., Peterzéns, P. G. and Andresen, A. F. *Acta Chem. Scand. A 32* (1978) 653.
19. Selte, K., Birkeland, L. and Kjekshus, A. *Acta Chem. Scand. A 32* (1978) 731.
20. Selte, K., Fjellvåg, H. and Kjekshus, A. *Acta Chem. Scand. A 33* (1979) 391.
21. Selte, K., Fjellvåg, H., Kjekshus, A. and Andresen, A. F. *Acta Chem. Scand. A 33* (1979) 727.
22. Fjellvåg, H. and Kjekshus, A. *Acta Chem. Scand. A 38* (1984) 563.
23. Fjellvåg, H. Selte, K. and Stave, F. E. *Acta Chem. Scand. A 38* (1984) 687.
24. Fjellvåg, H. and Kjekshus, A. *Acta Chem. Scand. A 38* (1984) 703.
25. Fjellvåg, H., Kjekshus, A. and Andresen, A. F. *Acta Chem. Scand. A 38* (1984) 711.
26. Fjellvåg, H. and Kjekshus, A. *Acta Chem. Scand. A 38* (1984) 719.
27. Fjellvåg, H., Kjekshus, A. and Andresen, A. F. *Acta Chem. Scand. A 39* (1985) 143.
28. Zięba, A., Fjellvåg, H. and Kjekshus, A. *J. Phys. Chem. Solids 46* (1985) 275.
29. Fjellvåg, H. and Kjekshus, A. *J. Solid State Chem. 59* (1985) 9.
30. Fjellvåg, H. and Kjekshus, A. *Acta Chem. Scand. A 40* (1986) XXX. (ACS No. 1854)
31. Fjellvåg, H., Kjekshus, A., Andresen, A. F. and Zięba, A. *J. Magn. Magn. Mat.* To be published.
32. Felcher, G. P. *J. Appl. Phys. 37* (1966) 1056.
33. Forsyth, J. B., Pickart, S. J. and Brown, P. J. *Proc. Phys. Soc. 88* (1966) 333.
34. Felcher, P. G., Smith, F. A., Bellavance, D. and Wold, A. *Phys. Rev. B 3* (1971) 3046.
35. Fjellvåg, H., Kjekshus, A., Zięba, A. and Foner, S. *J. Phys. Chem. Solids 45* (1984) 709.
36. Sheldrick, C. SHELX–Programme for Crystal Structure Determination (1976).
37. Hewat, A. W. The Rietveld Computer Program for the Profile Refinement of Neutron Diffraction Powder Patterns Modified for Anisotropic Thermal Vibrations, UKAERE Harwell Report RRL 73/897 (1973).
38. Rietveld, H. M. *J. Appl. Crystallogr. 2* (1969) 65.
39. Koester, L. and Yelon, W. B., In Yelon, W. B. Ed. *Neutron Diffraction Newsletter,* Missouri, 1983.
40. Pearson, W. B. *A Handbook of Lattice Spacings and Structures of Metals and Alloys,* Pergamon,

Oxford–London–Edinburgh–New York–Toronto–Paris–Braunschweig 1967, Vol. II.
41. Perkins, P. G., Marwaha, A. K. and Stewart, J. J. P. *Theoret. Chim. Acta 59* (1981) 569.
42. Selte, K. and Kjekshus, A. *Acta Chem. Scand. 27* (1973) 3195.
43. Endresen, K., Furuseth, S., Selte, K., Kjekshus, A., Rakke, T. and Andresen, A. F. *Acta Chem. Scand. A 31* (1977) 249.

Received June 7, 1985.